ELSEVIER

Journal of Photochemistry and Photobiology A: Chemistry 113 (1998) 53–64

Journal of Photochemistry and Photobiology A:Chemistry

Photogeneration of antiaromatic 8π xanthenide and thioxanthenide ('π-excessive') carbanions via excited-state carbon acid deprotonation and photodecarboxylation

Deepak Shukla, Peter Wan *

Department of Chemistry, Box 3065, University of Victoria, Victoria, British Columbia, Canada, V8W 3V6

Received 16 July 1997; received in revised form 7 October 1997

Abstract

The relatively facile generation of formally ground-state antiaromatic 8π xanthenide and thioxanthenide carbanions via excited-state C–H bond deprotonation and photodecarboxylation is reported. The aim of this work is to study the effect of heteroatoms (O and S) on the photogeneration of cyclically conjugated 4nπ-electron carbanion intermediates and comparing it with the corresponding photoreactions which generate the isoelectronic dibenzosuberenyl carbanion **23** from **22**, the first reported excited-state carbon acid. Quantum yields of proton incorporation in **1** and **4** were measured in aqueous ethanol and in CH_3CN using NaOH and ethanolamine as deprotonating bases, respectively. Primary kinetic isotope effect for C–H bond cleavage was measured by fluorescence quenching of **1** and **3** using ethanolamine as base (in CH_3CN) and found to be $k_H/k_D \approx 2$. The fluorescence quenching rate of **3** by ethanolamine, $k_q = 2.5 \times 10^7\ M^{-1}\ s^{-1}$, is two orders of magnitude smaller than that for dibenzosuberene (**22**) indicating that the 8π xanthenide (and thioxanthenide) carbanion is not as readily photogenerated as the isoelectronic dibenzosuberenyl carbanion (**23**). Estimated photodecarboxylation rate constants for xanthene-9-carboxylic acids **11** and **17** are an order of magnitude less than the corresponding rate constant for suberene-5-carboxylic acid (**24**), consistent with the lower rate (and possibly reduced driving force) for carbanion photogeneration for these isoelectronic heteroatom systems.

Keywords: Photodecarboxylation; Excited-state carbon acids; Photodeprotonation; Carbanions; Proton transfer

1. Introduction

The relative stability of molecules with cyclically conjugated π-systems and the relative energy content of transition states possessing cyclic π-electron arrays depend on the number of participating electrons and the topology of the orbital interactions, as described by Hückel's 4n + 2 Rule and the Woodward–Hoffmann Rules, respectively [1–3]. Consistent with experimental results, calculations of the resonance energy per π-electron for annulenes, relative to the corresponding acyclic conjugated planar systems, reveal that 4n + 2 electron systems (known as aromatic) are stabilized by resonance whereas the corresponding 4nπ electron systems (known as antiaromatic) are destabilized [4–6]. For example, theoretical studies of some prototype antiaromatic 4nπ-electron systems, e.g., cyclobutadiene [7] and cyclopropenyl carbanion [8,9], show that these systems do indeed have higher energy content than comparable open chain systems. However, the agreement observed between calculations and experimental results disappears on going to larger ring systems, viz., cyclooctatetraene, primarily due to nonplanarity of such systems [10,11]. Replacement of an ethylene group of cyclooctatetraene by a heteroatom bearing a nonbonding electron pair leads to the seven-membered heterotropilidines which are potential 8π-electron systems with antiaromatic character. Such heterotropilidenes, in contrast to cyclooctatetraene, exhibit pronounced antiaromatic destabilization and undergo valence isomerization to give hetero-σ-homobenzenes [12–15].

Indeed, the influence of heteroatoms on the phenomenon of aromaticity and antiaromaticity has been a subject of extensive theoretical and experimental work [16–21]. Of considerable interest in this area has been the effect of heteroatoms on the antiaromaticity of the systems possessing carbanionic center by the addition to a heteroatom unit (known as 'π-excessive' systems since there are more π electrons than there are atoms in the cyclic system) [22]. In general, such 'π-excessive' antiaromatic systems exhibit

* Corresponding author.

1010-6030/98/$19.00
PII S1010-6030(97)00298-0

reduced acidity of the starting materials and enhanced reactivity of the carbanions. For example, six-membered pyranyl ring systems consisting of a carbanionic center and a π-excessive heteroatom, viz., oxygen, have been shown to undergo ring contractive reorganization believed to be indicative of intrinsic antiaromatic instability of such systems [23]. However, the carbanions generated from related dibenzannelated systems, xanthene (**3**) and thioxanthene (**6**) (xanthenide and thioxanthenide carbanions, respectively) were found to be stable and did not undergo skeletal rearrangements [24–26]. In a related study, the ^{1}H NMR of the carbanions generated from a series of dibenzannelated systems, including xanthene (**3**) and thioxanthene (**6**), showed that the sulfur atom stabilizes the carbanion more effectively than oxygen in these carbanions [27].

Recent studies carried out by our group have shown that several dibenzannelated $4n\pi$ electron carbocation and carbanion intermediates are photochemically generated with much higher efficiency than their analogous $(4n+2)\pi$ electron or acyclic systems [28–34]. The facile photodecarboxylation of several dibenzannelated acetic acids [28] and the excited-state carbon acid behavior of dibenzosuberene (**22**)

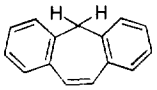

22

and related compounds [29–31] have all been attributed to the photogeneration of cyclically conjugated 8π-electron carbanion intermediates in these reactions, which are believed to be favored on the excited-state surface. The enhanced efficiency of photogenerating $4n\pi$-electron systems is not restricted to carbanionic intermediates. The conformational change observed in dibenzooxepin on photoexcitation, from a nonplanar to a more planar conformation, has been interpreted by us as due to attainment of an 8π-electron cyclic array in S_1 [35]. More recently, we have shown that C–H bond deprotonation of thioxanthenium salts in neutral CH_3CN gives rise to a long-lived ylide (formal carbanion) intermediate, the driving force of which is again believed to be due to formation of a cyclic 8π electron species on photolysis [36].

In this work, we report our study on the effects of heteroatoms (O and S) on the photogeneration of $4n\pi$ electron carbanion intermediates in dibenzannelated systems, via excited-state C–H bond heterolysis and via photodecarboxylation. We chose xanthene (**3**) and thioxanthene (**6**) systems for these investigations since the $4n\pi$ excessive carbanion intermediates of these systems, unlike pyranyl, are known not to undergo structural reorganization, and for which substantial data is available with respect to generating their carbanions in the ground state [24–26]. Furthermore, since these two carbanions are isoelectronic to the dibenzosuberenyl carbanion (**23**) a comparison of photoreactions which generate these intermediates should prove to be informative.

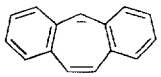

23

2. Experimental details

2.1. General

^{1}H NMR spectra were recorded on a Perkin-Elmer R32, Bruker WM250 or Bruker AMX360 instrument in $CDCl_3$. ^{13}C and ^{2}H NMR were acquired on either the WM250 or AM 360 instrument. UV–Vis spectra were recorded on a Perkin-Elmer Lambda 4B or a Pye-Unicam 800 spectrophotometer. IR spectra were recorded on a Perkin-Elmer 283 instrument. Mass spectra were obtained on a Finnigan 3300 mass spectrometer (EI or CI). High-resolution mass spectra (HRMS) were recorded on a Kratos Concept H (EI) instrument. Melting points were determined on a Koefler hot stage microscope and are uncorrected. GC analyses were performed on a Varian 3700 using an SE 54 capillary column and a Hewlett Packard 3390A integrator. Photolyses were carried out in Suprasil quartz cuvettes or 100/200 ml quartz tubes using a Rayonet RPR 100 photochemical reactor (254 or 300 nm lamps).

2.2. Materials

Dichloromethane (Van Waters and Rogers Ltd.), acetonitrile, and THF were distilled (CH_3CN over CaH_2; THF over K) prior to use while all other solvents (ACS reagent grade) were used without further purification. The D_2O used for solvent isotope studies and preparatory scale photolyses was 99.9% D (MSD Isotopes). Standard buffer solutions (Fisher Scientific) were used for product quantum yield experiments and fluorescence spectrophotometry. Solvents used for fluorescence studies were checked for spurious emission before use. Xanthone (**14a**), thioxanthone (**14b**), 9-xanthenol, xanthene-9-carboxylic acid (**11**), and 9-phenyl-9-xanthenol were obtained from Aldrich.

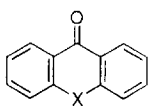

14a X = O
14b X = S

2.2.1. 9D-Xanthene (*1*)

To a stirred suspension of $LiAlD_4$ (0.047 g; 1.3 mmol) in THF (200 ml) at −4°C, $AlCl_3$ (0.35 g; 2.6 mmol) was slowly added under an inert atmosphere. The mixture was stirred for 10 min at 0°C and then xanthone (**14a**) (0.2 g; 0.7 mmol) was introduced. The reaction mixture was warmed to room temperature and then refluxed for 12 h. At the end

of reflux, the reaction was cooled in an ice bath and quenched with water (100 ml) followed by the addition of sufficient amount of 10% HCl solution to dissolve the suspension. The organic layer was separated and the aqueous layer was extracted with CH_2Cl_2. The combined organic layer was washed with water and dried over anhydrous $MgSO_4$. Removal of solvent in vacuo yielded crude **1** as a white solid (0.18 g, yield >95%), which was purified by recrystallization from 95% EtOH/H_2O; mp 102–104°C; ^{1}H NMR (90 MHz, $CDCl_3$) δ 7.10–7.50 (m, 8H, arom.); mass spectrum (CI) (*m/z*) 185 ($M^+ + 1$).

2.2.2. 9H,9D-Xanthene (2)

Treatment of 9-xanthenol with $LiAlD_4/AlCl_3$ in dry THF as in Section 2.2.1 afforded a white solid which was purified by recrystallization from EtOH/H_2O to obtain pure **2** (yield 77%); mp 103°C; ^{1}H NMR (250 MHz, $CDCl_3$) δ 4.05 (t, 1H, $J \sim 1.6$ Hz, Ar_2CHD), 7.0–7.4 (m, 8H, arom.); mass spectrum (CI) (*m/z*) 184 ($M^+ + 1$).

2.2.3. Xanthene (3)

Treatment of xanthone (**14a**) with $LiAlH_4/AlCl_3$ as in Section 2.2.1 afforded 9*H*-xanthene (**3**) as a white solid (yield >95%), which was purified by recrystallization from EtOH/H_2O; mp 100–101°C [lit. [37] mp 100.5°C]; ^{1}H NMR (90 MHz, $CDCl_3$) δ 4.0 (s, 2H, $ArCH_2Ar$), 7.10–7.50 (m, 8H, arom.); mass spectrum (CI) (*m/z*) 183 ($M^+ + 1$).

2.2.4. 9D-Thioxanthene (4)

Treatment of thioxanthone (**14b**) with $LiAlD_4/AlCl_3$ as in Section 2.2.1 afforded **4** as a white solid (yield >93%), which was purified by recrystallization from EtOH/H_2O; mp 147–148°C; ^{1}H NMR (90 MHz, $CDCl_3$) δ 7.10–7.50 (m, 8H, arom.); mass spectrum (CI) (*m/z*) 201 ($M^+ + 1$).

2.2.5. 9H,9D-Thioxanthene (5)

Treatment of 9-thioxanthenol (obtained by simple $LiAlH_4$ reduction of **14b**) as in Section 2.2.1 afforded **5** which was further purified by recrystallization from EtOH/H_2O; mp 146°C; ^{1}H NMR (250 MHz, $CDCl_3$) δ 3.82 (t, 1H, $J \sim 2$ Hz, Ar_2CHD), 7.1–7.5 (m, 8H, arom.); mass spectrum (CI) (*m/z*) 200 ($M^+ + 1$).

2.2.6. Thioxanthene (6)

Treatment of 9-thioxanthone (**14b**) with $LiAlH_4/AlCl_3$ as in Section 2.2.1 afforded **6** as a white solid (yield >90%), which was purified by recrystallization from EtOH/H_2O to obtain **6** as white crystalline material; mp 127–128°C [lit. [38] mp 128°C]; ^{1}H NMR (90 MHz, $CDCl_3$) δ 3.85 (s, 2H, $ArCH_2Ar$), 7.10–7.50 (m, 8H, arom.); mass spectrum (CI) (*m/z*) 199 ($M^+ + 1$).

2.2.7. 9-Phenyl-9D-xanthene (7)

Treatment of 9-phenyl-9-xanthenol with $LiAlD_4/AlCl_3$ as in Section 2.2.1 afforded crude **7** as a white solid (yield >95%), which was purified by recrystallization from 95% EtOH/H_2O; mp 144–145°C; ^{1}H NMR (90 MHz, $CDCl_3$) δ 6.95–7.30 (m, 13H, arom.); mass spectrum (EI) (*m/z*) 259 (M^+).

2.2.8. 9-Phenyl-9H-xanthene (8)

Treatment of 9-phenyl-9-xanthenol with $LiAlH_4/AlCl_3$ as in Section 2.2.1 afforded crude **8** which was purified by recrystallization from EtOH/H_2O to obtain **8** as a white crystalline solid (yield >95%); mp 144°C [lit. [39,40] mp 145°C]; ^{1}H NMR (90 MHz, $CDCl_3$) δ 5.25 (s, 1H, Ar_3CH), 6.95–7.30 (m, 13H, arom.); mass spectrum (EI) (*m/z*) 258 (M^+).

2.2.9. 9-Phenyl-9H-thioxanthene (9)

Treatment of 9-phenyl-9-thioxanthenol (prepared as described in Section 2.2.10) (2.0 g, 6.9 mmol) with $LiAlH_4/AlCl_3$ as in Section 2.2.8 yielded **9** as a white solid (1.8 g; yield >93%), which was purified by recrystallization from EtOH/H_2O; mp 99–100°C [lit. [41] mp 99°C]; ^{1}H NMR (90 MHz, $CDCl_3$) δ 5.25 (s, 1H, Ar_3CH), 6.90–7.55 (m, 13H, arom.); mass spectrum (EI) (*m/z*) 275 (M^+).

2.2.10. 9-Phenyl-9D-thioxanthene (10)

To the stirred solution of **14b** (1.0 g, 4.72 mmol) in dry THF (125 ml) at 0°C, 2.0 M solution of PhLi (2.5 M, 5.0 mmol) was introduced slowly with a syringe. The reaction mixture was stirred at room temperature for 12 h and then carefully quenched with water. The organic layer was separated out and the aqueous layer was extracted with CH_2Cl_2. The combined organic layers were washed with water, dried over $MgSO_4$ and CH_2Cl_2 removed to afford a pale yellow solid which was recrystallized from hexane/ether mixture to give the desired alcohol (9-phenyl-9-thioxanthenol) as a white crystalline solid; mp 107°C [lit. [42] mp 109°C]; ^{1}H NMR (90 MHz, $CDCl_3$) δ 2.30 (s, 1H, –OH), 6.90–7.50 (m, 11H, arom.), 7.90–8.10 (m, 2H, *peri* arom. H); mass spectrum (EI) (*m/z*) 291 (M^+). Treatment of this material (2.0 g, 6.9 mmol) with $LiAlD_4/AlCl_3$ in dry THF (175 ml) afforded **10** as a white solid (1.8 g; yield >93%), which was purified by recrystallization from EtOH/H_2O; mp 100–101°C; ^{1}H NMR (90 MHz, $CDCl_3$) δ 7.90–7.55 (m, 13H, arom.); mass spectrum (EI) (*m/z*) 276 (M^+).

2.2.11. 9,9′-Bixanthyl (12)

A solution of **3** (200 mg) and *p*-nitrobenzoic acid (800 mg) in 100 ml H_2O and 100 ml CH_3CN (pH adjusted to 12) was irradiated at 350 nm for 2.5 h. The reaction mixture was extracted with CH_2Cl_2 and the solvent removed in vacuo, to afford a crude material which was purified by preparative TLC (silica; 2:1 hexanes–CH_2Cl_2) to afford **12**, which was recrystallized from 95% EtOH, mp 201–204°C (lit. [43] 205–207°C), ^{1}H NMR δ 7.30–6.55 (m, 16H, ArH), 4.18 (s, 2H, ArCH); ^{13}C NMR δ 115.9, 121.9, 122.6, 128.1, 129.2, 153.1; MS (EI) *m/z* 362 (M^+).

*2.2.12. 9D-Xanthene-9-carboxylic acid (**13**)*

Treatment of 9*D*-xanthene (**1**) (2.0 g; 10 mmol) in dry THF (175 ml) with *n*-BuLi (2 M, 7 ml, 14 mmol) and CO_2, yielded crude **13** as a white solid on work-up (1.64 g; yield > 65%). The crude material was purified by recrystallization from 95% EtOH to afford **13** as a white crystalline material; mp 224–226°C; ^{1}H NMR (90 MHz, acetone-d_6) δ 7.20–7.60 (m, 8H, arom.); IR (KBr, cm^{-1}) ν 3400–3200 (broad, O–H str.), 1698 (strong, C=O str.), 1254 (strong, C–O str.); mass spectrum (EI) (*m/z*) 227 (M^+).

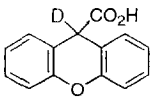

13

*2.2.13. 9H-Thioxanthene-9-carboxylic acid (**15**)*

Treatment of 9*H*-thioxanthene (**6**) (2.0 g; 10 mmol) as in Section 2.2.12 yielded crude **15** as a white solid (1.64 g; yield > 65%), which was purified by recrystallization from 95% EtOH to afford **15** as a white crystalline material; mp 224–226°C [lit. [44] mp 227°C]; ^{1}H NMR (90 MHz, acetone-d_6) δ 5.10 (s, 1H, Ar_2CH), 7.20–7.60 (m, 8H, arom.); IR (KBr, cm^{-1}) ν 3400–3200 (broad, O–H str.), 1698 (strong, C=O str.), 1254 (strong, C–O str.); mass spectrum (CI) (*m/z*) 243 ($M^+ + 1$).

*2.2.14. 9-Phenylthioxanthene-9-carboxylic acid (**16**)*

Treatment of 9-phenyl-9*H*-thioxanthene (**9**) (3.0 g, 10.1 mmol) as in Section 2.2.12 afforded a light pink solid (1.75 g, yield > 50%) which was recrystallized from 95% EtOH to yield pure **16** as a white crystalline solid; mp 162 ± 1°C; ^{1}H NMR (90 MHz, acetone-d_6) δ 6.95–7.50 (m, 13H, arom.); IR (KBr, cm^{-1}) 3400–3200 (broad, O–H str.), 1700 (strong, C=O str.), 1260 (strong, C–O str.); mass spectrum (CI) (*m/z*) 319 ($M^+ + 1$); HRMS, calc. for $C_{20}H_{14}O_2S$ 318.3969, obs. 318.3967.

*2.2.15. 9-Phenylxanthene-9-carboxylic acid (**17**)*

Treatment of 9-phenyl-9*H*-xanthene (**8**) (2.0 g, 7.76 mmol) as in Section 2.2.12 yielded a solid which was recrystallized from 95% EtOH to give **17** as a white crystalline solid (1.2 g; yield 55%): mp 168–169°C; ^{1}H NMR (90 MHz, acetone-d_6) δ 7.0–7.40 (m, 13H, arom.); IR (KBr, cm^{-1}) 3450 (broad, O–H str.), 1690 (strong, C=O str.), 1266 (strong, C–O str.); mass spectrum (CI) (*m/z*) 303 ($M^+ + 1$); HRMS, calc. for $C_{20}H_{14}O_3$ 302.3323, obs. 302.3321.

2.3. Product studies

2.3.1. General procedure

Samples (50–80 mg) were dissolved in the solvent or solvent mixture and placed in a quartz tube (100 or 200 ml), cooled with a cold finger (running tap water), and continuously purged with a stream of argon via a long syringe needle. After photolysis, the solutions were quenched with 5–10% HCl and extracted with CH_2Cl_2. For the carboxylic acids, care was made to ensure that the pH was ≈ 1–2 before extraction. The combined organic extracts were dried over $MgSO_4$ and solvent removed in vacuo and photolysate analyzed by GC/MS and ^{1}H NMR. Xanthenes **1** and **3**, thioxanthenes **4** and **6**, 9-phenyl-substituted analogues **7**–**10** did not show thermal proton/deuterium exchange and carboxylic acids **11**, **15**, **16** and **17** did not thermally decarboxylate under the reaction conditions employed in this study; complete recovery of the substrate was achieved under these conditions on work-up. The identity of all photoproducts was determined by comparison with authentic samples made above.

*2.3.2. Thermal generation of 9-xanthenide carbanion (**18-H**)*

To a stirred solution of 9*H*-xanthene (**3**, 0.1 mol) in THF (100 ml), excess of *n*-BuLi (2.0 M, 5.0 mol) was added under N_2. The reaction mixture was refluxed for 20 min to give a deep red solution of the 9-xanthenide carbanion (**18-*H***). To record the absorption spectrum, a portion (200–500 μl) of this solution was transferred to a quartz cuvette containing 2.5 ml of dry THF in a glove bag. The UV–Vis absorption spectrum showed a strong band at λ_{max} ~ 590 nm due to the carbanion which disappeared on exposure of the solution to air or moisture. That **18-*H*** was indeed generated was shown by quenching the solution with CO_2(g), which afforded xanthene-9-carboxylic acid (**11**) in > 75% yield. Using the Förster cycle [45–47], and $\Delta E_{0,0}$ ~ 44 kcal mol^{-1} for **18** (based on the absorption band at 590 nm) and pK(S_0) ≈ 30 for **3** [48], a pK(S_1) ≈ −2 for **3** was calculated.

*2.4. Estimation of ground-state pK_a for carboxylic acids **11**, **15** and **17***

The pK_a's of some of the diarylacetic acids studied in this work were estimated by titrating a 10^{-3} M solution of carboxylic acid dissolved in 4:1 H_2O–CH_3CN (deionized H_2O) with a standardized NaOH solution. A standard glass electrode with Ag/AgCl reference was employed for hydronium ion concentrations. End points were determined by a curve-fitting procedure, and the pK_a was taken as the pH at half-neutralization.

2.5. Quantum yields measurements

Quantum yields (Φ) of proton/deuteron exchange in **1**, **4**, **3**, and **6** were measured on an optical bench using an Oriel 200W Hg lamp and an Applied Physics monochromator set at λ_{ex} = 280 nm with slits of 7.0 nm. The light intensity at the excitation wavelength 280 nm was measured before and after each photolysis by employing potassium ferrioxalate actinometry according to the method of Hatchard and Parker [49]. Samples were prepared by taking 50 μl of stock solution (10^{-4} to 10^{-3} M) of substrate and diluting it to 3.00 ml with the appropriate solvent mixture in a Suprasil quartz

cuvette. The concentration of the each substrate in the cuvette solutions was adjusted to an absorbance ~2.0 at the excitation wavelength. The solutions were purged with a stream of argon for 5 min prior to and during the photolysis (usually 30–45 min). The conversions to photoproducts were kept between 10–15% in all cases. After irradiation the photolysate was transferred into a test tube and acidified to pH ≈ 7 with 5% HCl, and extracted with CH_2Cl_2. The photolysate was analyzed by GC/MS (CI mode) to determine the percent deuterium/protium exchanged products formed. The percentage of exchange product(s) formed were calculated from the mass spectrum after correcting for the natural abundance of ^2H and ^{13}C.

Quantum yields of formation of the corresponding decarboxylated products for **11**, **15**, **16** and **17** were measured also using $\lambda_{ex} = 280$ nm. A CH_3CN solution of the substrate (0.6 ml; 5×10^{-4} M) in a quartz cuvette was diluted with H_2O (2.4 ml of appropriate pH) was purged with a stream of argon for 5 min prior to and during the photolysis (usually 1–10 min). The reaction mixture was transferred to a test tube and acidified to pH ≈ 1 (with aqueous 5% HCl), and extracted with CH_2Cl_2. The organic fractions were then combined and washed with H_2O (pH ≈ 1; 2 × 10 ml), dried over $MgSO_4$ and filtered. Each solution was then injected with 50 μl of a stock solution of an external standard of appropriate molarity (viz., dibenzosuberene (**22**) in the case of **11** and **15**; 9-phenyl-9*H*-thioxanthene (**9**) in the case of 9-phenylxanthene-9-carboxylic acid (**17**); and 9-phenyl-9*H*-xanthene (**8**) in the case of 9-phenylthioxanthene-9-carboxylic acid (**16**)) and evaporated to ca. 200 μl before being injected into the GC for analysis. In the case of carboxylic acid **11**, only the quantum yields for formation of **3** were measured (product **12** had a very long retention time which prevented an accurate determination of its quantum yield of formation).

2.6. Steady-state fluorescence and lifetime measurements

Steady-state fluorescence measurements were carried out on a Perkin-Elmer MPF-66 spectrophotometer at ambient temperature. Samples (≈ 10^{-6} M) were prepared in 3.0 ml quartz cuvettes and purged with argon prior to measurement. Fluorescence quantum yields were determined by comparing the integrated emission band of the substrate with those of an appropriate secondary standard. Secondary standards for fluorescence quantum yields measurements were so chosen as to maximize their spectral overlap with the emission band of the sample. Dibenzofuran ($\Phi_f = 0.53$ [50]) and diphenyl ether ($\Phi_f = 0.03$ [50]) were chosen as secondary fluorescence standards due to similarities in structure with the compounds under study and reasonable spectral overlap in fluorescence emission.

Fluorescence lifetimes were measured using the single photon counting technique, on a Photon Technology International (PTI) LS-1 instrument using a H_2 flash lamp as the excitation source. Solutions of the samples (O.D. < 0.2) were purged with argon before each measurement. All decays were analyzed using software supplied by PTI and were first-order.

3. Results and discussion

3.1. Proton/deuteron exchange studies

Photolysis of 9*D*-xanthene (**1**) or 9*D*-thioxanthene (**6**) in 1:1 H_2O–CH_3CN at 300 nm for 1 h did not result in any observable exchange of deuterium at C_9 and the starting materials were recovered (in case of **1**, a 10–20% yield of a previously documented photoisomerization as well as very minor side products were observed [51]). However, photolysis in the presence of aqueous NaOH (using EtOH as cosolvent) resulted in observable exchange of deuterium. Thus, photolysis of an argon purged solution of **1** (10^{-3} M) in 1:1 (1 M NaOH/H_2O)–EtOH (300 nm; 75 min) gave a mixture which was analyzed by ^1H NMR and GC/MS. The ^1H NMR showed the appearance of a diagnostic broad triplet (deuterium with a nuclear spin of one also has a quadrupole moment) at δ 4.05 ($J \sim 1$–2 Hz) (Fig. 1) which was assigned to 9*D*,9*H*-xanthene (**2**). The photoisomerization of **1** observed in neutral solution [51] is now absent indicative of a more facile competing reaction, viz. excited-state carbon acid deprotonation. GC/MS analysis of the photolysate showed that **2** (10 ± 2%) was formed along with a small amount of **3** (3 ± 2%) (Eq. (1)).

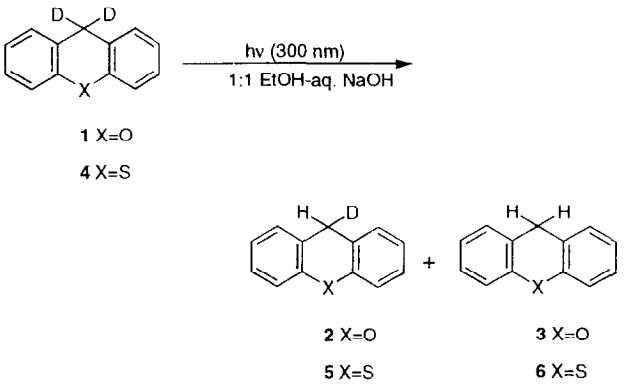

(1)

A similar irradiation of a solution of **4** also resulted in mono- and di-deuterium exchanged products at the benzylic position to give **5** (≈ 18%; a diagnostic triplet at δ 3.82 ($J \approx 1$–2 Hz)) and 9*H*-thioxanthene (**6**) (≈ 7%; singlet at δ 3.85) (Eq. (1)).

Photolysis of **1** and **4** in 1:1 (1 M NaOH/H_2O)–EtOH at 300 nm with analysis of photolysate at regular intervals by ^1H NMR and GC/MS clearly shows (Figs. 2 and 3) that at short photolysis times, monodeuterated **2** and **5** are the primary photoproducts which reacts further via a secondary photoreaction, to yield photoproducts **3** and **6**, respectively.

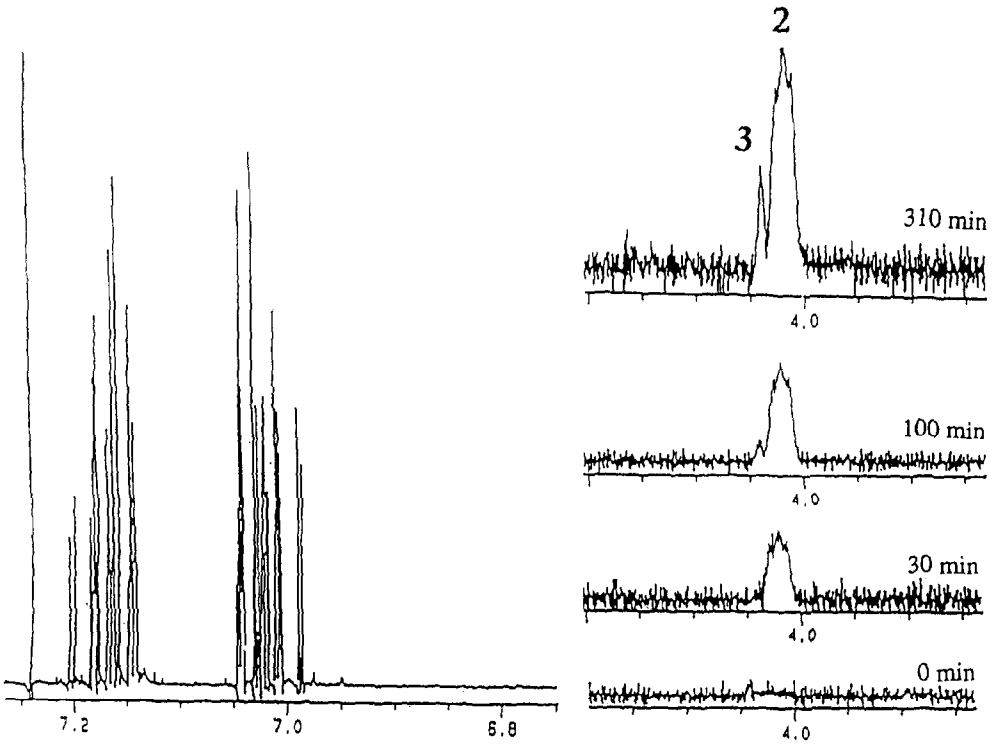

Fig. 1. ^{1}H NMR (360 MHz) spectrum showing incorporation of proton at the benzylic position on photolysis of 9*D*-xanthene (**1**) in 1:1 (1 M NaOH/H_2O)–EtOH at various photolysis times. The aromatic signals remain unchanged throughout the photolysis.

Photolysis of 9*H*-xanthene (**3**) in 1:1 (1 **M** NaOD/D_2O)–EtOD also resulted in exchange, viz. formation of monodeuterated **2** as the major product at low conversions along with a small amount of **1** (Eq. (2)).

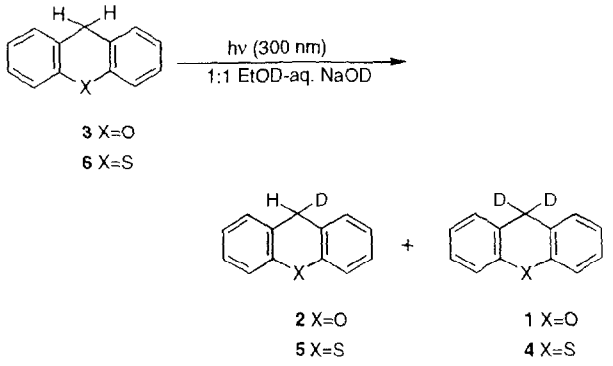

(2)

A similar photolysis of 9*H*-thioxanthene (**6**) resulted in the formation of **5** along with small amount of **4** (Eq. (2)). The possibility of a residual amount of deuterium incorporation into the benzene ring of **3** and **6** was carefully examined by ^{2}H NMR. A solution of **3** in 1:1 (1 M NaOD/D_2O)–EtOD was irradiated for 1 h and the photolysate examined by ^{2}H NMR in CD_2Cl_2 with acetone-d_6 as internal standard. The spectrum of the product mixture showed a strong peak at $\delta \approx 4.1$ due to mono- and di-deuteration (due to both **1** and **2**; unresolved peak) at the C_9 position. No peaks were

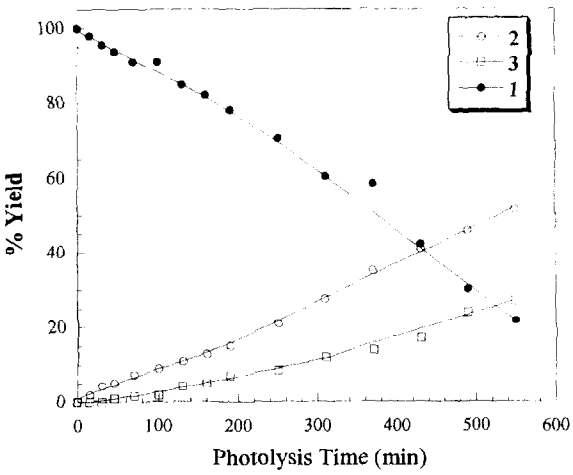

Fig. 2. Plot of yield of exchange vs. photolysis time for **1** in 1:1 (1 M NaOH/H_2O)–EtOH.

observed in the aromatic region of the ^{2}H NMR spectrum, clearly establishing that the deuterium exchange takes place exclusively at C_9. A similar experiment with **6** gave the same result. Due to the high expense of using deuterated bases and solvents (e.g., NaOD and D_2O), most of the exchange studies were subsequently carried using labelled (deuterated) substrates in normal (nondeuterated) solvents which are further described below.

Deuterium exchange of **1** and **4** was also observed when these systems were irradiated in CH_3CN in the presence of ethanolamine as base, giving cleaner reactions and higher conversions than photolysis in (NaOH/H_2O)–EtOH. For

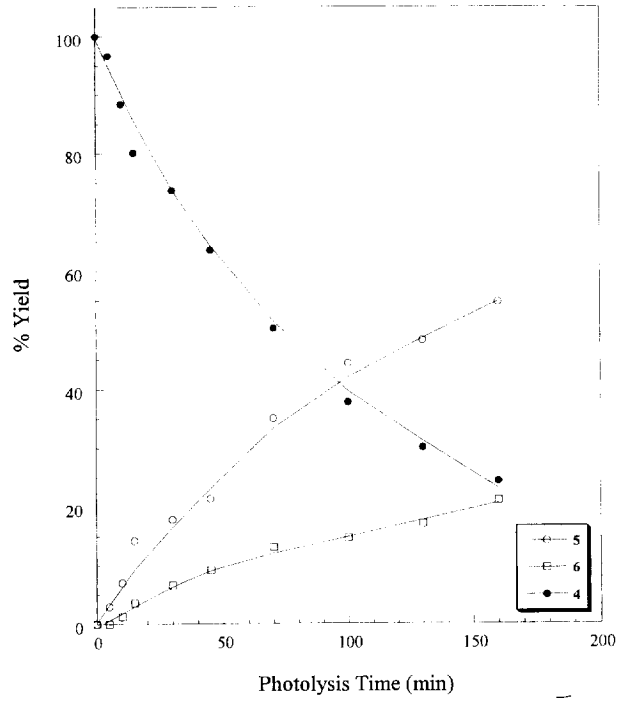

Fig. 3. Plot of yield of exchange vs. photolysis time for **4** in 1:1 (1 M NaOH/H_2O)–EtOH.

example, photolysis of a CH_3CN solution of **1** (10^{-3} M, 5 min) in the presence of 5 M ethanolamine resulted in the formation of **2** (≈60%) and **3** (≈24%). Since photolysis of **1** and **4** in neutral H_2O–EtOH or 100% CH_3CN did not result in any exchange, it indicates that these systems require the use of NaOH or ethanolamine as deprotonating base, unlike the behavior of dibenzosuberene (**22**) in which exchange was readily observable in neutral H_2O (CH_3CN as cosolvent) [29].

Quantum yields for formation of mono-deuterium exchanged products **2** and **5** (from **1** and **4**, respectively) were measured and found to increase with increasing concentration of NaOH and ethanolamine. In 1:1 (NaOH/H_2O)–EtOH, quantum yields were low, ranging from ≈0.00021 in 1 M NaOH to ≈0.00035 in 5 M NaOH for formation of **2** from **1**. However, quantum yields for exchange were higher when ethanolamine was used (in CH_3CN). Table 1 gives the quantum yields for mono-deuterium incorporation (formation of **2** and **5**) on photolysis at various concentrations of ethanolamine in CH_3CN. All quantum yields of exchange are significantly lower than those measured for the parent excited-state carbon acid, **22** [29,31], and suggests less reactive systems in **1** and **4** (**3** and **6**).

3.2. Photodecarboxylation

Photolysis of **11** in 4:1 H_2O–CH_3CN (pH≈8; 10 min) gave **3** and 9,9′-bixanthyl (**12**) (Eq. (3)).

Table 1
Quantum yields of deuterium exchange of **1** and **4** (formation of **2** and **5**) in CH_3CN with ethanolamine as base[a]

[Ethanolamine][b]	Φ(**2**)	Φ(**5**)
1.0	0.0074	0.0056
2.0	0.0098	0.0074
3.0	0.014	0.0090
4.0	0.017	0.010
5.0	0.020	0.014

[a]Quantum yields were measured on an optical bench with λ_{ex} = 280 nm and potassium ferrioxalate actinometry [49]; yields determined by GC/MS; estimated errors ±15%.
[b]Concentration of ethanolamine in CH_3CN.

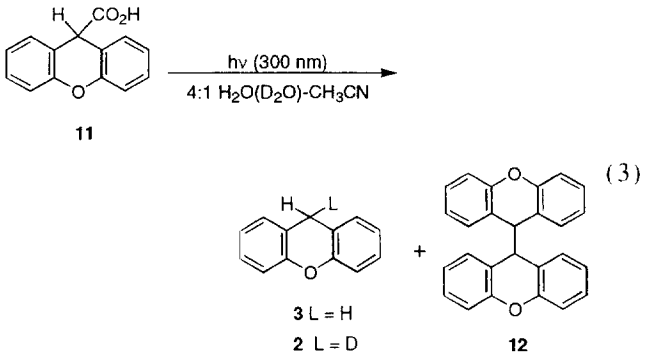

(3)

In an earlier study we have reported that photolysis of **3** in aqueous CH_3CN solution results in the formation of a minor amount of **12**, via the xanthenyl radical (**20**) [51]. However, a control photolysis of **3** in 4:1 H_2O–CH_3CN (pH≈8) under the reaction conditions employed for **11** did not give **12**, ruling out the possibility that **12** is formed via secondary photolysis of **3**. Furthermore, analysis of the reaction mixture at various conversions in the photolysis of **11** showed the presence of both **3** and **12** at short photolysis times (ca. 30 s; very low conversion (<10%)), consistent with the proposal that both are primary photoproducts.

Photolysis of **11** in oxygen saturated solutions under conditions where extensive decarboxylation occurred resulted in formation of **3** and 9-xanthone (**14a**) along with a trace amount of 9,9′-bixanthyl (**12**). Control experiments in which both **3** and **12** were independently photolyzed in oxygen saturated aqueous CH_3CN (ca. 90 min) gave only traces (<1%) of **14a**, ruling out the possibility that **14a** could have formed via direct photolysis of **3** or **12**. In separate control experiments where **11** was photolyzed in oxygen and argon saturated aqueous CH_3CN, the yield of **3** remained unchanged. However, in oxygen saturated solutions, ketone **14a** was formed at the expense of **12**. These results suggest that both **12** and **14a** originate from a common precursor. Furthermore, photolysis of **11** in 4:1 D_2O–CH_3CN (neutral pD) readily afforded **2** and **12** (Eq. (3)). Interestingly, the ^1H NMR and mass spectrum of the photolysate showed no deuterium was

incorporated in **12**. This result again shows that **12** does not originate from **3** (**2**).

The possibility that the proton at C_9 of **11** was undergoing photoexchange (there is no thermal exchange) with the solvent D_2O prior to the decarboxylation was checked by irradiating 9*D*-xanthene-9-carboxylic acid (**13**) in 4:1 H_2O–CH_3CN: no deuterium loss was observed in recovered **13**. Furthermore, photolysis of **3** in 4:1 D_2O–CH_3CN also did not result in deuterium exchange at the benzylic position (a reaction that has been observed in more basic solution, vide supra) ruling out the possibility that deuterated **2** could have arisen from secondary photolysis of **3**.

Photolysis of carboxylic acid **15** in 4:1 H_2O–CH_3CN (pH ≈ 8) cleanly afforded 9*H*-thioxanthene (**6**) (Eq. (4)).

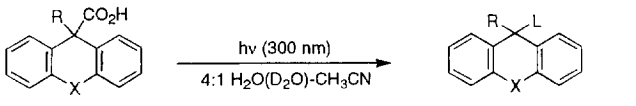

15 R = H; X = S
16 R = Ph; X = S
17 R = Ph; X = O

5 R = H; L = D; X = S
6 R = H; L = H; X = S
7 R = Ph; L = D; X = O
8 R = Ph; L = H; X = O
9 R = Ph; L = H; X = S
10 R = Ph; L = D; X = S

(4)

A similar photolysis of **15** in 4:1 D_2O–CH_3CN (p*D* ≈ 9) resulted in clean formation of the corresponding monodeuterated product **5** (Eq. (4)). Again, the possibility that the observed deuterium in **5** could have resulted from secondary photolysis of **6** (vide supra) was ruled out by irradiating **6** under conditions employed for the photodecarboxylation of **15**, which did not result in any observable deuterium exchange. 9,9′-Bithioxanthyl (sulfur analog of **12**) was not observed in these photolyses.

The presence of a phenyl substituent at the C_9 position had little effect on the photodecarboxylation. Thus, photolysis of both **16** and **17** in 4:1 H_2O–CH_3CN (pH ≈ 8) resulted in efficient formation of **9** and **8**, respectively. A similar photolysis of in 4:1 D_2O–CH_3CN resulted in the formation of deuterated **10** and **7**, respectively. However, the pH of the medium had a significant effect on the efficiency of photodecarboxylation for all compounds studied. Table 2 gives the quantum yields for product formation via photodecarboxylation of the carboxylic acids studied. It is evident that in aqueous solutions with pHs < pK_a (the estimated pK_a of **11** and **17** are 4.0 and 4.5, respectively) photodecarboxylation does not take place and indicate that only the carboxylate ions are reactive (the chromophore is not changed to any significant extent on ionization of the carboxylic acid for these compounds). Quantum yields were lower in D_2O (Table 2, entry 4), giving solvent isotope effects on quantum yield, $\Phi(H_2O)/\Phi(D_2O) \approx 1.2$–1.3. It is interesting to note that xanthenecarboxylic acids **11** and **17** photodecarboxylate with higher quantum yields than thioxanthenecarboxylic

Table 2
Quantum yields of photodecarboxylation of xanthene and thioxanthene carboxylic acids in aqueous solution[a]

	Φ_p[b]			
pH[c]	**11**[d]	**17**	**15**	**16**
1.0	0.00	0.00	0.00	0.00
2.0	0.00	0.00	0.00	0.00
4.0	0.074	0.060	0.038	0.046
7.0	0.30 (0.24)[e]	0.28 (0.22)[e]	0.18 (0.14)[e]	0.22 (0.17)[e]
9.0	0.33	0.30	0.20	0.23
10.0	0.33	0.32	0.22	0.26
12.0	0.34	0.33	0.23	0.26

[a]Quantum yields were measured on an optical bench with $\lambda_{ex} = 280$ nm and potassium ferrioxalate actinometry [49]; yields determined by GC/MS using an external standard; estimated errors ± 15%.
[b]Quantum yield for formation of the corresponding decarboxylated product from the indicated carboxylic acid starting material (e.g., **3** from **11**).
[c]pH of the 4:1 H_2O–CH_3CN mixture directly measured using a pH meter (adjusted using NaOH or dilute H_2SO_4, as required).
[d]Refers to formation of **3** only since **12** had a very long retention time on the GC.
[e]In 4:1 D_2O–CH_3CN.

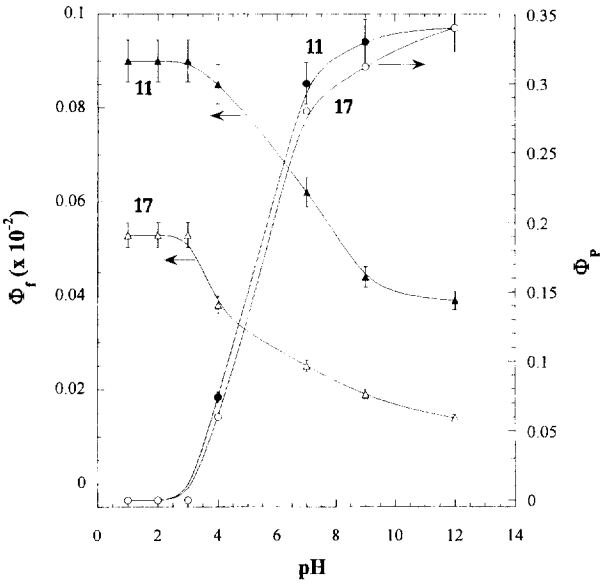

Fig. 4. Plot of Φ_p (for photodecarboxylation) and Φ_f vs. pH for carboxylic acids **11** and **17**.

acids **15** and **16** at all pHs (Table 2), but are all less than the reported quantum yield for **24** ($\Phi = 0.60$; all pHs) [28].

Consistent with photodecarboxylation via carboxylate ions, the fluorescence quantum yields of **11** and **17** were lower in aqueous solutions in which these acids photodecarboxylate extensively. Thus, the fluorescence quantum yield of **11** in 100% CH_3CN was $\Phi_f = 0.022 \pm 0.002$ (relative to biphenyl ether ($\Phi_f = 0.03$) [50]), a solvent where **11** does not photodecarboxylate, whereas in 4:1 H_2O–CH_3CN (pH 7.0), where **11** efficiently photodecarboxylates ($\Phi_p = 0.30$), $\Phi_f \approx$ 0.0062. The corresponding 9-phenyl derivative **17**, although

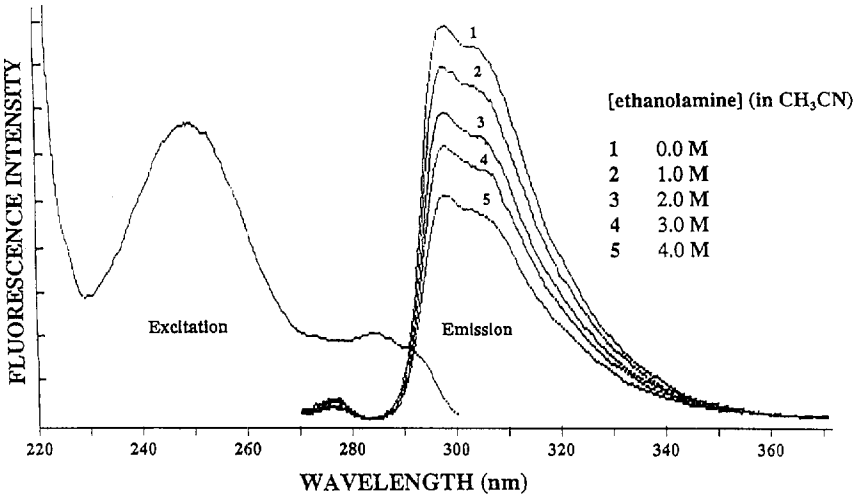

Fig. 5. Fluorescence quenching of **3** by added ethanolamine in CH_3CN (λ_{ex} = 260 nm).

weakly fluorescent (Φ_f = 0.0082 in CH_3CN), also exhibited similar behavior. A plot of Φ_p and Φ_f vs. pH, shown in Fig. 4, is clearly consistent with reactivity of the carboxylate ion form of these compounds.

3.3. Kinetics of excited-state carbon acid behavior

The kinetics of excited-state carbon acid deprotonation in CH_3CN using ethanolamine as deprotonating base was quantitatively investigated by both steady state fluorescence and lifetime measurements, using the method documented by us for **22** and related compounds [29–31]. In accord with the primary C–H (D) bond cleavage in S_1, the fluorescence of **1** and **3** ($\Phi_f = 0.23 \pm 0.02$ in CH_3CN; a previously reported $\Phi_f = 0.05$ [51] is incorrect) were quenched by added ethanolamine in CH_3CN. Fig. 5 shows the fluorescence quenching of **3** in CH_3CN by added ethanolamine. Fluorescence lifetimes (τ) of **1** and **3** in CH_3CN were also reduced by added ethanolamine. However, **3** was quenched faster than **1** in both steady state and lifetime measurements. Quenching rate constant (k_q) were determined by Stern–Volmer analysis using both steady state fluorescence and lifetimes. Fig. 6 shows a representative Stern–Volmer plot for quenching using fluorescence lifetimes of **1** and **3** in CH_3CN by ethanolamine. A good agreement, within experimental errors, between the k_q's obtained by steady state fluorescence quenching ($k_q(\mathbf{1}) = 1.2 \times 10^7\ M^{-1}\ s^{-1}$; $k_q(\mathbf{3}) = 2.5 \times 10^7\ M^{-1}\ s^{-1}$) and lifetimes ($k_q(\mathbf{1}) = 1.1 \times 10^7\ M^{-1}\ s^{-1}$; $k_q(\mathbf{3}) = 2.2 \times 10^7\ M^{-1}\ s^{-1}$) is consistent with a dynamic quenching mechanism for interaction of ethanolamine with the excited singlet states of **1** and **3** [52]. Furthermore, fluorescence quenching rate constants of **1** and **3** by ethanolamine in CH_3CN exhibited a significant primary isotope effect, $(k_H/k_D) \approx 2.00$, which is consistent with the ethanolamine-assisted heterolytic C–L (L=H and D) bond cleavage in S_1. The fluorescence of both **4** and **6** ($\Phi_f = 0.008$ [50]) was very weak preventing a systematic quenching study; the presence of the sulfur atom no doubt increases the intersystem crossing rates ($\Phi_{ISC} = 0.78$ for **6** [50]) for these compounds and hence a low Φ_f.

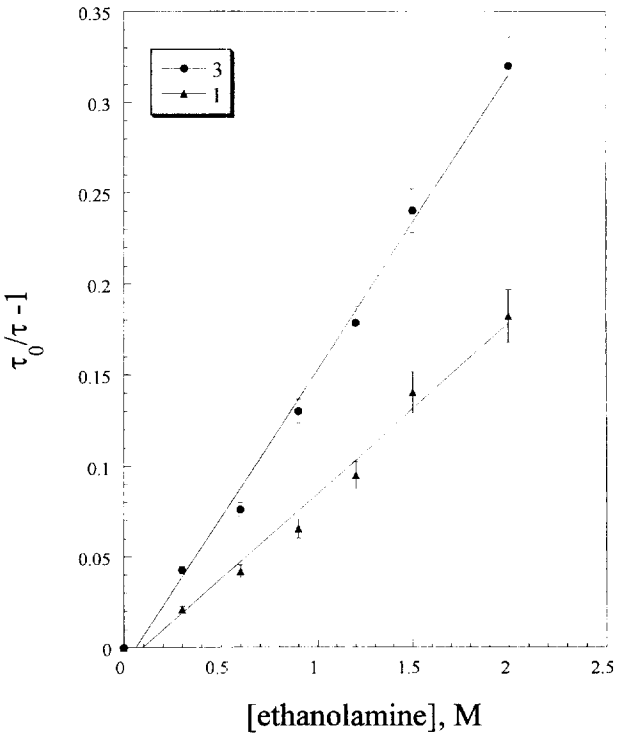

Fig. 6. Stern–Volmer plot using lifetimes for ethanolamine quenching of **1** and **3** ($\tau_0(\mathbf{1}) = 7.72 \pm 0.04$ ns; $\tau_0(\mathbf{3}) = 7.59 \pm 0.03$ ns).

3.4. Mechanism of excited-state carbon acid deprotonation

The results presented for carbon acid deprotonation are consistent with base assisted C–L (L=H or D) bond cleavage in S_1. A generalized reaction mechanism using **1** as starting material and ethanolamine (RNH_2) as base is shown in Scheme 1. Abstraction of the deuteron by the base RNH_2 from the benzylic position of **1** on photoexcitation gives the intermediate xanthenide carbanion **18-*D*** (the corresponding sulfur system **4** would give **19-*D***). The carbanion **18-*D*** may be hydrogen bonded to the departing RNH_2D^+ and may re-bond to the intermediate carbanion resulting in no net exchange (internal return). However, exchange of the depart-

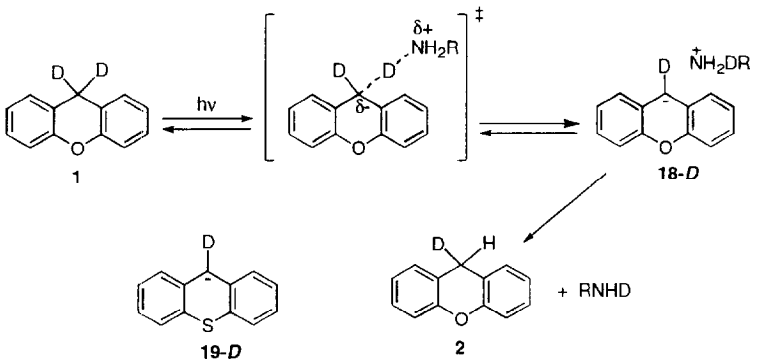

Scheme 1.

ing deuteron with a proton from RNH_2D^+, and subsequent protonation of the intermediate carbanion **18-*D*** results in an overall exchange at the benzylic position of **1**, to give monodeuterated product **2**. The primary kinetic isotope effect of $k_H/k_D \approx 2$ observed in fluorescence quenching data of **1** and **3** by ethanolamine is consistent with ethanolamine-assisted benzylic C–H vs. C–D bond cleavage as the primary photochemical step. Since internal return of the abstracted deuteron leads to not net exchange, the observed quantum yields of exchange are expected to be low. This expectation is further supported by the following observations. Φ_f of **1** in the nonreactive solvent CH_3CN is 0.23 ± 0.02. In the presence of 2.0 M ethanolamine, Φ_f drops to 0.19 ± 0.02. However, the observed monodeuterium exchange quantum yield in this solvent is 0.0098 (Table 1, entry 2). If it is assumed that the decrease in Φ_f is completely due to the reaction of excited **1** via heterolytic deuteron abstraction from the benzylic C–D position, then out of about 100 deprotonated molecules only 20 undergo exchange. This indicates that internal return of the deuteron is the major reaction pathway of photogenerated carbanion **18-*D***.

Deprotonation of **3** ($pK(S_0) \approx 30$ [48]) in the ground state is difficult and strongly basic conditions are required (e.g., KNH_2 in liquid ammonia [24–26]). However, on irradiation, both of **3** and **6** undergo deprotonation under relatively mild conditions confirming that these compounds become much more acidic in S_1. The enhanced excited-state acidity of **3** and **6** is predictable using the Förster cycle [45–47], which gave $pK_a(S_1) \approx -2$ for **3** (see Section 2). Similar calculations for fluorene (**21**) gave $pK_a(S_1) \approx -8$ [47]. However, fluorene (**21**),

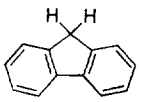

21

which forms a $(4n+2)$ π-electron carbanion intermediate, is not known to undergo photochemical exchange of the benzylic protons under any condition [47,29]. A reasonable explanation is that the activational barrier for carbon acid deprotonation on the excited-state surface is strongly controlled by the electron count (4 n vs. 4 n + 2) of the cyclic transition state, analogous to ground-state reactions which give rise to transition states with cyclically conjugated π systems [3]. In the ground state, an electron count of $4n+2$ is favoured in the transition state (as well giving rise to the more stable product) [1–3]. However, on the excited-state surface, carbon acid deprotonation is observed for only those transition states with an $4n$ electron count, although in principle, the 'driving force' (as calculated by the Förster cycle [45–47]) is substantial ($pK_a(S_1) < 0$) whether it has $4n$ or $4n+2$ electrons.

3.5. Mechanism of photodecarboxylation

A general mechanism for photodecarboxylation is proposed in Scheme 2 using **11** (carboxylate ion form) as the model compound. Two possible extremes with respect to the nature of the primary decarboxylation step may be envisaged. Simple loss of CO_2 gives rise to a free carbanion **18-*H***, which can pick up a proton from solvent to give **3** or loose an electron to give the xanthenyl radical **20**, and hence **12** and **14a** (the latter in the presence of oxygen). Oxidation product **14a** could also arise via direct attack of **18-*H*** by oxygen, which cannot be ruled out with the data available. Another possibility is that loss of CO_2 is concerted with proton transfer from solvent, to give **3** in one step. This latter pathway is consistent with the observed solvent isotope effects ($\Phi(H_2O)/\Phi(D_2O) \approx 1.2$–$1.3$ (Table 2, entry 4). Clearly, either extreme is incorrect as they are inconsistent with all the data at hand. We propose that either the decarboxylation step involves both processes, or a single mechanism in which there is significant hydrogen bonding from the solvent to the carbanion, thus consistent with the formation of **20** and **14a** and the observed solvent isotope effect.

It is not clear at this time why only **11** gave 'dimer' **12** whereas none of **15-17** gave detectable amounts of the corresponding 'dimer' product. It may be that the parent xanthenide carbanion **18-*H*** is the most destabilized of these π-excessive anions and is prone to undergo electron loss.

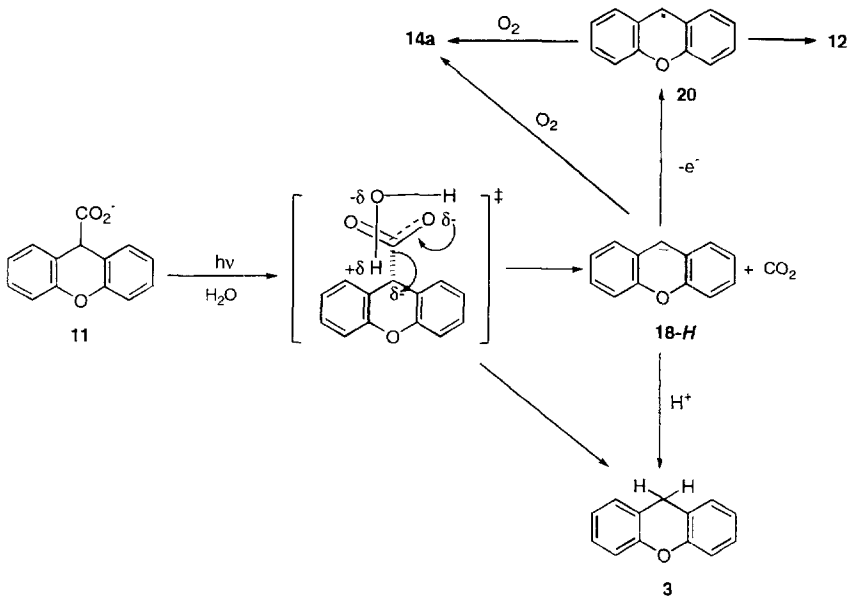

Scheme 2.

This explanation seems reasonable since the corresponding carbanions from **15–17** would all be more stabilized than the parent **18-*H***: they either have a sulfur atom and/or a phenyl group, both of which will have an additional stabilizing effect on the benzylic negative charge.

4. Summary

This study has demonstrated the generality of photogenerating dibenzannelated 8π carbanion systems using heteroatom systems based on the xanthene (**3**) and thioxanthene (**6**) ring system, via carbon acid deprotonation and decarboxylation. The reactions are less efficient compared to the parent dibenzosuberene systems **22** and **24** but go nevertheless under the appropriate conditions.

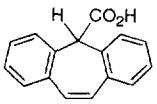

24

In contrast, the corresponding thermal reaction are observed only under much more drastic reaction conditions. A recent theoretical study [53] on the excited-state carbon acid behavior of **22** and related compounds suggests that the driving force for reaction can be explained by symmetry arguments using orbital and/or configurational correlation diagrams in addition to explaining why more flexible derivatives do not react via carbon acid dissociation. It would be of interest to test this theoretical treatment for the systems studied in this work especially since the xanthene (**3**) and thioxanthene backbone (**6**) are more planar than dibenzosuberene (**22**) in the ground and Franck–Condon states.

References

[1] E. Hückelvalign[ch, Z. Phys. 70 (1931) 204.
[2] E. Hückelvalign[ch, Z. Phys. 76 (1932) 628.
[3] R.B. Woodward, R. Hoffmann, The Conservation of Orbital Symmetry, Verlag Chemie, Weinheim, 1970.
[4] B.A. Hess, L.J. Schaad, J. Am. Chem. Soc., 93 (1971) 305, 2413.
[5] B.A. Hess, L.J. Schaad, J. Org. Chem. 36 (1971) 3418.
[6] B.A. Hess, L.J. Schaad, C.W. Holyoke, Tetrahedron, 28 (1972) 3657, 5299.
[7] G. Maier, Angew. Chem., Int. Ed. Engl. 13 (1974) 425.
[8] R. Breslow, Acc. Chem. Res. 6 (1973) 425.
[9] R. Breslow, Pure Appl. Chem. 28 (1971) 111 and references cited therein.
[10] R.A. Raphael, in: D. Ginsburg (Ed.), Nonbenzenoid Aromatic Compounds, Wiley-Interscience, New York, 1959, p. 465.
[11] G. Schroder, Cyclooctatetraen, Verlag Chemie, Weinheim, 1965.
[12] K. Hafner, Angew. Chem., Int. Ed. Engl. 3 (1964) 165.
[13] E. Vogel, H. Gunther, Angew. Chem., Int. Ed. Engl. 6 (1967) 385.
[14] G. Maier, Angew. Chem., Int. Ed. Engl. 6 (1967) 402.
[15] L.A. Paquette, Angew. Chem., Int. Ed. Engl. 10 (1971) 11.
[16] M.J.S. Dewar, A.J. Harget, N. Trinajstic, S.D. Worley, Tetrahedron 26 (1970) 4504.
[17] B.A. Hess Jr., L.J. Schaad Jr., C.W. Holyoke Jr., Tetrahedron 28 (1972) 3657.
[18] B.A. Hess Jr., L.J. Schaad Jr., J. Am. Chem. Soc. 95 (1973) 3907.
[19] M.J. Cook, A.R. Katritzky, P. Lunda, in: A.R. Katritzky, A.J. Boulton, (Eds.), Advances in Heterocyclic Chemistry, Vol. 17, Academic Press, New York, 1974, p. 255.
[20] A.G. Anastassiou, Acc. Chem. Res. 9 (1976) 453.
[21] A.G. Anastassiou, H.S. Kasmai, Adv. Heterocyclic Chem. 23 (1978) 55.
[22] A. Albert, Heterocyclic Chemistry: An Introduction, Althone, London, 1968.
[23] R.R. Schmidt, Angew. Chem., Int. Ed. Engl. 14 (1975) 581.
[24] A.G. Anastassiou, H.S. Kasmai, Angew. Chem., Int. Ed. Engl. 19 (1980) 393.
[25] A.G. Anastassiou, H.S. Kasmai, Angew. Chem., Int. Ed. Engl. 19 (1980) 43.
[26] A.G. Anastassiou, H.S. Kasmai, M.R. Saadein, Tetrahedron Lett. (1980) 3743.

[27] H.S. Kasmai, J.F. Femia, L.L. Healy, M.R. Lauria, M.E. Lansdown, J. Org. Chem. 52 (1980) 5461.
[28] E. Krogh, P. Wan, J. Am. Chem. Soc. 114 (1992) 705.
[29] D. Budac, P. Wan, J. Org. Chem. 57 (1992) 887.
[30] P. Wan, D. Budac, M. Earle, D. Shukla, J. Am. Chem. Soc. 112 (1990) 8048.
[31] D. Budac, P. Wan, J. Photochem. Photobiol. A: Chem. 98 (1996) 27.
[32] P. Wan, D. Budac, E. Krogh, J. Chem. Soc., Chem. Commun. (1990) 255.
[33] P. Wan, E. Krogh, J. Am. Chem. Soc. 111 (1989) 4887.
[34] E. Krogh, P. Wan, Can. J. Chem. 68 (1990) 1725.
[35] D. Shukla, P. Wan, J. Am. Chem. Soc. 115 (1993) 2990.
[36] D. Brousmiche, D. Shukla, P. Wan, J. Chem. Soc., Chem. Commun. (1997) 709.
[37] N. Latif, J. Org. Chem. 27 (1962) 846.
[38] C. Graebe, Justus Liebigs Ann. Chem. 263 (1891) 1.
[39] H.E. Ungnade, E.F. Kline, E.W. Crandall, J. Am. Chem. Soc. 75 (1953) 333.
[40] M.H. Hubacher, J. Am. Chem. Soc. 65 (1943) 1655.
[41] B.E. Maryanoff, J. Am. Chem. Soc. 97 (1975) 2718.
[42] V.M. Gomberg, L.H. Cone, Justus Liebigs Ann. Chem. 376 (1910) 201.
[43] I.T. Badejo, R. Karaman, A.A. Pinkerton, J.L. Fry, J. Org. Chem. 55 (1990) 4327.
[44] R.R. Burtner, J.W. Cusic, J. Am. Chem. Soc. 65 (1943) 1582.
[45] J.F. Ireland, P.A.H. Wyatt, Adv. Phys. Org. Chem. 12 (1976) 131.
[46] L. M. Tolbert, in: E. Buncel, T. Durst (Eds.), Comprehensive Carbanion Chemistry, Part C, Elsevier, Amsterdam, 1987.
[47] E. Vander Donckt, J. Nasielski, P. Thiry, J. Chem. Soc., Chem. Commun. (1969) 1249.
[48] R. Stewart, The Proton: Applications to Organic Chemistry, Academic Press, Orlando, 1985.
[49] C.G. Hatchard, C.A. Parker, Proc. R. Soc. London, Ser. A 235 (1956) 518.
[50] S.L. Murov, I. Carmichael, G.L. Hug, Handbook of Photochemistry, 2nd edn., Marcel Dekker, New York, 1993.
[51] C.G. Huang, D. Shukla, P. Wan, J. Org. Chem. 56 (1991) 5437.
[52] J.R. Lakowicz, Principles of Fluorescence Spectroscopy, Plenum, New York, 1983.
[53] H.M. Steuhl, M. Klessinger, Angew. Chem., Int. Ed. Engl. 33 (1994) 2431.